Journal Home Page: https://sjes.univsul.edu.iq/

Research Article:

Shear Performance of GFRP Reinforced Concrete Beams Without Transverse Reinforcement

Zhin Othman Ahmed [1,a,*]
Alan Saeed Abdulrahman [2,a]
[a] University of Sulaimani, College of Engineering, Civil Engineering Department, KR,Iraq

Article Information

Article History:
Received: January, 18th , 2026
Accepted : April 11, 2026
Available online: April , 2026

Keywords:
GFRP bars, shear strength, stirrups, dowel action, tensile reinforcement ratio.

About the Authors:
Corresponding author:
Zhin Othman Ahmed Rasul
E-mail: zhin.rasul@univsul.edu.iq
Researcher Involved:
Dr. Alan Saeed Abdulrahman
E-mail: alan.Abdulrahman@univsul.edu.iq

DOI https://doi.org/10.17656/sjes.10202

Abstract

This study investigates the influence of glass fiber-reinforced polymer reinforcement bars on the shear capacity of simply supported concrete beams without web reinforcement and to investigate the dowel effect of this reinforcement. To determine the effects of concrete compressive strength, type of reinforcement, and reinforcement ratio on shear behavior, an experimental program was conducted on 12 beam samples, comprising six conventionally steel-reinforced beams and six beams. reinforced with GFRP bars. There were three different tensile reinforcement ratios (low, medium, and high) in each subgroup. Both the beams that have reinforced with GFRP or steel bars were designed to have theoretically the same tension forces (A_sF_y its equivalent from the GFRP properties) which resulted in comparable flexural capacity and two concrete compressive strengths. The experimental findings revealed that the shear capacity of GFRP-reinforced beams was approximately 36% less than that of steel-reinforced beams at low reinforcement ratios, 28% at intermediate reinforcement ratios, and 16% at high reinforcement ratios. And the enhancement of concrete compressive strength from 40 MPa to 55 MPa (38%) increased the shear capacity of GFRP-reinforced beams more significantly than that of beams reinforced with conventional steel. Also, the ACI code-440.11-22 formulae significantly underestimates the shear capacity, with an average ratio of experimental to predicted shear capacity of approximately 2.0 for both concrete compressive strength values that were chosen.

1. Introduction

There is a growing demand for structural materials that are lightweight, cost effective, and environmentally suitable, while also providing high strength, durability, and minimal maintenance in aggressive environments. Over the past decades, fiber-reinforced polymers (FRPs) have gained significant attention as a means of meeting these requirements. Due to their high strength, resistance to corrosion, and durability FRP materials have been used successfully in new construction and rehabilitation applications. Consequently, FRPs have become a strengthening technique for many structural applications and an important topic in the structural engineering research and practice [1-6]. Conventional reinforced concrete structures in harsh environments often suffer durability problems, primarily corrosion of steel reinforcement. Corrasion may lead to cracking, spalling of the concrete covering, and reduction in the effective steel cross sections which can compromise structural safety and serviceability. To address these challenges, GFRP Bars have been introduced as an alternative to conventional steel reinforcement. GFRP provides high resistance to corrosion and high tensile strength, [7, 8]. The behavior of beams reinforced with fiber-reinforced polymer (FRP) bars under flexural loading has been studied by numerous researchers [9-11]. However, regarding the shear carrying capacity of structural concrete members reinforced with FRP, there is a lack of agreement and understanding. In FRP reinforced concrete beams without transverse reinforcement, shear resistance is generally attributed to

several mechanisms, including aggregate interlock, shear resistance of un-cracked concrete compression zone, shear resistance of FRP stirrups, residual tensile stress across the cracks, dowel action of longitudinal reinforcement and arch action. Because FRP bars have a relatively low elastic modulus, the flexural reinforcement's radius affects the depth and width of the crack, as well as the dowel action. [12]. The shear behavior of GFRP reinforced beams differs from that of steel of steel reinforced beams due to the different mechanical properties of GFRP bars, In particular when used as longitudinal reinforcement. GFRP bars exhibit limited shear resistance, which reduces their ability to transfer shear forces acting perpendicular to the bar [13]. The relatively low transvers shear resistance of GFRP bars reduces the dowel action that typically contributes to the shear strength of steel reinforced concrete beams. As a result, the shear capacity of GFRP reinforced beams is often underestimated when dowel action is neglected, leading to overly conservative design predictions. In recent years, several researchers have studied conventional steel and GFRP bars on beams having different cross sections without web reinforcement. The longitudinal reinforcement ratio was an important factor affecting the shear capacity of the GFRP-reinforced concrete beam. Melo et al. 2002 [14] Tested the shear resistance of two simply supported GFRP reinforced concrete beams without web reinforcement using concrete strength varying from 53.8 to 70 MPa. having a/d=2.5. The results showed that increasing the longitudinal ratio from 1.6-3.26% had improved the shear strength by 57% as with a linear relationship between normalized shear strength and reinforcement ratio $\boldsymbol{\rho}$%. Koray et al. 2002 [7] Tested nine large-scale reinforced concrete beams with nominal concrete compressive strength 34.5 MPa without transverse reinforcement. Three types of FRP reinforcement, two GFRP (ribbed and sand-coated). The longitudinal reinforcement ratio of the GFRP varied from 0.92 to 1.92%. They found that the shear strength increased with increasing longitudinal reinforcement percentage, but at different rates. The rate of increase of sand-coated GFRP was 24%, while that for the ribbed one was 58%. Gross et al. 2003 [15] investigated the effect of reinforcement ratio (ρ_f) .It was found that the longitudinal reinforcement ratio had little effect on the concrete shear-strength. Ashour 2006 [16] examined the effective of beam depth and the amount of GFRP reinforcement using twelve simply supported concrete beams reinforced with GFRP bars without shear reinforcement. Their result showed that shear capacity of GFRP-reinforced beams increased by 140% when the reinforcement ratio was increased from 0.45% to 1.15%. Under reinforced beams failed in flexure due to GFRP bar rupture, whereas over reinforced beams exhibited a different failure mode. The linear trend was observed by El-Sayed et al. 2005 [17] Through evaluating the shear capacity of five simply supported GFRP reinforced concrete slabs subjected to four-point loading. The results showed that the specimens reinforced by GFRP bars exhibited larger deformations at ultimate fracture-load. In addition, Abed et al., (2012) [18], reported that shear strength is proportioned to the square root of the GFRP reinforcement (ρ). The shear strength of GFRP-reinforced beams increases 70% when the reinforcement ratio increases from 0.92% to 1.84% . At the same reinforcement ratio, the shear strength of GFRP-reinforced beams is 50% higher than that of their steel-reinforced counterparts [18], [19]. This was approved by Krall and Polak 2019 [3], Ali et al. 2014 [19] and by El-Sayed et al. 2006b [20]. Results for Kaszubska et al. 2017 [21] , tested on T-beams, indicate that shear strength in beams with two layers of longitudinal reinforcement increased by about 37% when the reinforcement ratio increased from 1.02% to 1.85%. The effect of concrete compressive strength was studied by several researchers [15] through testing simply supported beams reinforced with GFRP bars without web reinforcement. They concluded that shear capacity is significantly affected by the concrete compressive strength. Since the elastic models of FRP bars are lower than that of the steel bar, so the beam's axial stiffness is reduced, and its mid-span deflection is increased. Additionally, a few wide and long cracks tend to develop rapidly [12, 22, 23]. Based on best knowledge of the authors, no body conducted any study related to the investigating of the impact of dowel action of GFRP bars on shear strength of concrete beams without web reinforcement and that was stated on the ACI code-440.11-22 chapter 22 page 161 were they mentioned explicitly "The contribution of longitudinal GFRP reinforcement in terms of dowel action has not been determined".

2. Objective of the Study

This paper will investigate the impact of dowel action on the shear strength of concrete beams without web reinforcement through experimental work. The matrix will involve two compressive strengths, fixed aggregate size, fixed cross section, different ratios of reinforcement as well as comparable beams that were reinforced with conventional steel for comparison purposes. The beams were designed to have flexural capacities similar to conventional reinforced concrete beams in order to compare the shear behavior of beams with the same flexural capacity but different reinforcement types and GFRP bar sizes.

3. Experimental Program

3.1 Materials and Concrete Mixes

In this study, two concrete strength grades were used approximately 40 MPa and 55MPa, the actual compressive strengths *f'c* were determined by testing standard 100×200mm cylinder at 28 days age. Common Portland cement (CEM I 42.5 R), natural sand and natural coarse aggregate with a nominal maximum size

of 9 mm were present. A high-performance superplasticizer at 1% cement weight was used in 55 MPa concrete to enhance workability and to minimize the water-cement ratio. Trial mixes were made to arrive at concrete mix proportions that produced the target strengths and sufficient workability. The beams were cast using companion specimens from the same batches to determine the concrete's mechanical properties. Table 1 presents the properties of aggregate, and Table 2 shows the mix proportion of the concrete.

3.2 Beam Specimens

Twelve simply supported reinforced concrete beams were cast and tested under a single concentrated load at mid-span. All beams had dimensions i.e., 2000 mm long, 300 mm wide, and 400 mm deep. The beams were divided into two main groups based on reinforcement type, GFRP bar and steel bar. Each group was further divided according to the concrete compressive strength (40 MPa and 55 MPa), and within each subgroup had three different tensile reinforcement ratios (low, medium, and high). Both GFRP and steel-reinforced beams were designed to carry theoretically the equivalent tensile forces ($Asfy$ or their equivalent from the GFRP properties), resulting in comparable flexural capacity. Beams reinforced with steel had ρ_{e1}=0.0037, ρ_{e2}=0.0102, and ρ_{e3}=0.014, While for GFRP reinforced beams, ρ_{e1}=0.0022, ρ_{e2}=0.00586, and ρ_{e3}=0.0102. In the low-reinforcement-ratio cases, 10 mm diameter bars were used, and in the medium- and high-reinforcement-ratio cases, 14 mm bars were used, as shown in Table 3. The mechanical properties of the reinforcement used in this study are as follows: steel bars were deformed with a yield strength of 420 MPa, and modulus of elasticity of 200000 MPa while the sand-coated GFRP bars had an ultimate tensile strength of 1200 MPa and a modulus of elasticity of 55,000 MPa, as provided by the manufacturer. The properties of GFRP bars are shown in table 4.To encourage shear-dominated behavior, all beams were reinforced only in the tension zone, and no stirrups or compression reinforcement were provided as shown in figure 1. Both the beams reinforced with GFRP or steel bars were designed to have the same theoretical tension forces. Figure 2 is the flow chart of the beams group.

3.3 Instrumentation

Strain and deflection were monitored for each beam. Four strain gauges were installed on the longitudinal reinforcement of the shear spans of both sides of the beam. To measure compressive strain, one concrete strain gauge was placed at the midspan, 50mm below the top of the surface as shown in Figure 3. The vertical deflection was measured with an LVDT at midspan of each beams.

3.4 Test set-up and loading Process

A self-supporting loading frame with an 800 kN capacity was used to test all beams. A load cell was placed at mid-span with a single-point load being applied, and that load cell was connected to a data acquisition unit where load, strain and displacement were simultaneously recorded. The beams were supported with a 150 mm distance at both ends, and the clear span was 1700 mm. Monotonically loading at a low rate was applied. At a point where a visible crack was formed, the loading was stopped to record crack propagation and note the relevant load. It was repeated until failure was reached. Figure 4 is the beam under load.

3.5 Theoretical Evaluation and Design Codes

Moreover, experimental shear capacities compared with corresponding theoretical shear strength evaluated using ACI 440,IR-22 design equations. This comparison was used to evaluate the accuracy, reliability, and conservatism of the current design provisions of GFRP-reinforced concrete beams without transvers reinforcement. According to this analysis, the objective of the study was to identify potential drawbacks of the current design guidelines and provide information to help enhance the prediction models for the shear strength of concrete beams reinforced with GFRP bars.

4. Results and Discussion

4.1 Beam Test Results

The beams were all selected to fail in shear, and this shear dominated behavior was effectively observed in all the specimens. Although the response during the initial loading phase was similar in all beams, the behavior exhibited after the cracking was very different. In particular, the difference was noted in the patterns of crack formation, failure modes, and characteristics of load-deflection. These variations in the final shear capacity were largely controlled by three experimental variables, the compressive strength of concrete ($f'c$), the reinforcement type (Steel vs. GFRP), and the reinforcement ratio (ρ).

4.2 Crack Pattern and Mode of Failure

The crack patterns in the beam specimens varied with the concrete's compressive strength and the reinforcement arrangement. The first flexural cracks tended to occur at mid-span, where the point loads were applied, and to propagate vertically towards the compression zone as the load increased. With further loading, inclined cracks formed in the shear spans and ultimately controlled the process of failure as shown in Figure 5. Two primary failure modes were observed, shear-flexural failure and diagonal tension (shear tension) failure. The fundamental difference between these two modes lies in the crack initiation and the progression of the failure: while shear-flexural failure begins with vertical cracks that slowly turn diagonal, diagonal tension occurs suddenly with a diagonal crack forming directly in the shear span. Shear-flexural failure was found in a small set of low-reinforcement ratio GFRP-reinforced beams in which flexural cracks

evolved progressively into inclined shear cracks. This progressive transition allows for more observation of the crack growth compared to the other mode. The other beams collapsed through diagonal tension, which consists of the sudden extension of a dominant inclined crack resulting in a sudden failure. Unlike the shear-flexural mode, diagonal tension failure occurs without the prior development of vertical flexural cracks in the shear zone, making it a much more abrupt event. The failure modes found are in line with the brittle character of shear failure, especially in GFRP-reinforced members. Table 5 presents the crack patterns and failure modes of the beams.

4.3 Load–Deflection Behavior

The load-deflection behavior of the tested beams under load provides important insights into stiffness, ductility, and the overall structural response of the beams under shear-dominated loading. The maximum load carried by each beam, and the associated deflection are indicated in Table 6. The load-deflection curves of the tested beams depend on the compressive strength of the concrete (40 MPa and 55 MPa), reinforcement ratio, and the type of reinforcement. In general, a higher reinforcement ratio increases the load-carrying capacity of both steel-reinforced and GFRP-reinforced beams and reduces deflections during failure. Overall, the GFRP-reinforced beams exhibited larger deflections and more gradual load-deflection behavior without yielding, whereas the steel-reinforced beams were less flexible and had reduced deflections because the steel could yield in a ductile manner. Additionally, increasing concrete compressive strength improved the load capacity for both reinforcement types, with a more pronounced effect on the GFRP-reinforced beams. Furthermore, at the same reinforcement ratios (almost the same theoretical flexural strength), the shear capacity of the steel-reinforced beam was higher, implying that the dowel action of GFRP beams is less significant. Figure 6 shows the load-deflection curves, A) for the 40 MPa group, and B) for the 55 MPa group beams.

4.4 Influence of main parameters on the shear strength

The experimental result clearly indicate that concrete compressive strength, reinforcement type, and reinforcement ratio are key parameters influencing the shear capacity of reinforced concrete beams. Variations in these parameters had major impacts on cracking behavior, failure mechanisms, and ultimate shear resistance. In general , the shear capacity of both steel- and GFRP-reinforced beams increased with higher concrete compressive strength, however the magnitude of improvement depended on the reinforcement configuration. Steel-reinforced beams consistently exhibited higher shear strength and lower deflections due to the increased stiffness and yielding capacity of steel reinforcement, whereas GFRP-reinforced beams were more sensitive to changes in concrete strength and reinforcement ratio because of their linear-elastic response and lower modulus of elasticity bars.

4.4.1 Impact of Concrete Compressive Strength

One of the most effective parameters determining the shear behavior of reinforced concrete beams is concrete compressive strength. An increase in concrete compressive strength typically enhances shear resistance by increasing aggregate interlock, increasing compressive stress transfer across cracks, and delaying diagonal crack propagation. For steel-reinforced beams, as shown in Figure 7, increasing the concrete compressive strength from 40 MPa to 55 MPa (an increase approximately 38%) lead to in a modest increase in shear capacity. Specifically, the shear strength increased by about 8% for beams with low steel reinforcement ratios and by approximately 12% for beams with moderate reinforcement ratios. However, in beams with high steel reinforcement ratios, no considerable increase in shear capacity was realized. This behavior implies that at higher reinforcement ratios, the shear response is increasingly controlled by reinforcement stiffness and strain compatibility rather than by the concrete's strength itself. Conversely, the effect of concrete compressive strength was stronger in GFRP-reinforced beams, particularly at medium and high reinforcement ratios, as shown in Figure 8. For these beams, increasing the concrete strength from 40 MPa to 55 MPa resulted in shear strength increases of approximately 17% and 14% for ρe2 and ρe3, respectively. This indicates that with a sufficient GFRP reinforcement ratio, concrete strength can enhance shear resistance by increasing the contribution of dowel action.

4.4.2 Impact of Type of Reinforcement (Steel vs. GFRP)

The type of longitudinal reinforcement is important for the shear behavior of reinforced concrete beams due to the inherent mechanical differences between steel and GFRP bars. Steel reinforcement has high stiffness, ductility, and yield capacity, which enhances shear resistance through improved dowel action. Conversely, GFRP reinforcement is linear elastic until rupture and has a significantly lower modulus of elasticity, resulting in increased crack and a lesser contribution to shear transfer mechanisms. These variations were clearly evident in the experimental results at both levels of concrete strength. For beams with 40 MPa concrete steel reinforced beams exhibited superior shear performance at all reinforcement ratios. Compared to steel-reinforced beams, the shear capacity of GFRP-reinforced beams was lower by approximately 36%, 28%, and 16% at low, moderate, and higher reinforcement ratios respectively. The trends of the two types of reinforcement were similar as the reinforcement ratio increased, but the absolute shear

capacities of the steel-reinforced beams were greater. These results are shown in Figure 9. This trend was also observed in the 55 MPa concrete group. The shear capacity of GFRP-reinforced beams was reduced by approximately 58%, 25%, and only 4% at low, moderate and higher reinforcement ratios respectively when compared to steel-reinforced beams as shown in figure 10. This indicates that, with increased reinforcement ratio, the effectiveness of GFRP reinforcement in shear resistance increases. These findings showed that the dowel action of beams reinforced with low and moderate ratios of GFRP tensile bars is about 30% lower than that of their counterparts in conventional steel-reinforced beams. Nevertheless, with close-to-maximum reinforcement ratios, the performance difference between steel and GFRP beams is relatively small, indicating that GFRP reinforcement may be used to achieve shear capacities very similar to those of steel when applied in adequate amounts. The significance of appropriate reinforcement design is emphasized in the case of GFRP bars.

4.4.3 Impact of Reinforcement Ratio

One of the most critical factors affecting the shear strength of reinforced concrete beams is the reinforcement ratio, which determines the ability of longitudinal reinforcement to resist diagonal cracking and mobilize dowel action. An increase in the reinforcement ratio tends to enhance crack control, stiffness, and total shear resistance. This pattern was observed across both reinforcement types and across the two levels of concrete compressive strength, although the magnitude of improvement was significantly greater for steel than for GFRP reinforcement. In the 40 MPa concrete group, the steel-reinforced beam showed a definite and steady increase in shear strength as the reinforcement ratio increased. When the reinforcement ratio increased from the lowest (ρ_{e1}) to the medium, shear strength increased by 25%; from medium to about maximum, it increased by 18%, and from ρ_{e1} to maximum, it increased by 47%. These results indicate that steel reinforcement is effective in delaying diagonal cracking and enhancing shear resistance (Figure 11). In GFRP-reinforced beams with 40 MPa concrete, the reinforcement ratio had a more pronounced effect. The shear capacity increased by approximately 40% at low reinforcement ratios and by 38% at moderate ratios. At near-maximum reinforcement ratios, the shear capacity increased by about 94%, indicating a substantial improvement in performance when sufficient GFRP reinforcement was provided. As shown in figure 12. The same behavior was observed with the 55 MPa concrete group. Figure 13 shows the results of steel beams in 55 MPa concrete strength group. Increasing the steel reinforcement ratio from (ρ_{e1}) to (ρ_{e2}) increased the shear capacity by approximately 30%, and a further increase to (ρ_{e3}) produced a total increase of about 37%. It was also observed that GFRP-reinforced beams in this category also displayed a pronounced increment in shear strength with a higher reinforcement ratio. The measured results indicate that increasing the GFRP reinforcement ratio from (ρ_{e2}) to (ρ_{e3}) increased the shear strength by approximately 35%. Results for GFRP beams in 55 MPa concrete strength are shown in Figure 14. In general, experimental findings show that the reinforcement ratio plays an important role in the shear strength of both steel- and GFRP-reinforced beams. Steel reinforcement can support a continuous increase in shear capacity at moderate reinforcement ratios, whereas GFRP reinforcement requires higher reinforcement ratios to match performance. These results highlight the importance of selecting appropriate reinforcement ratios when designing GFRP-reinforced concrete beams to provide satisfactory shear resistance.

4.5 Comparison with Design Codes

The experimental findings in this study were compared to the shear strength predictions provided by the American and Canadian design codes, namely, ACI 318-25[24] , ACI 440.1R-22 [25], CSA S806-12 [26] and CSA A23.3-24[27]. The aim of this comparison was to evaluate the accuracy, reliability, and degree of conservatism of existing design provisions when applied to reinforced concrete beams without transverse reinforcement whether reinforced with traditional steel bars or GFRP bars. The comparison assesses the effects of reinforcement type, reinforcement ratio, and concrete compressive strength on the predictive power of the selected codes. It also evaluates the ability of both design standards to realistically capture the shear behavior and ultimate load capacity of the tested beams studied.

4.5.1 Predicted versus Experimental Shear Capacity

The shear capacity of the test beams was measured according to the provisions of the four selected designed codes. All codes determine the concrete contribution to shear resistance, Vc, using all empirical or semi-empirical formulations developed on reinforced concrete members without shear reinforcement. However, the design codes differ in their assumptions requiring shear transfer mechanisms, the contribution of longitudinal reinforcement, and strain effects. ACI 318-25[24] provides empirically calibrated shear equations for steel-reinforced concrete members with a minimum specified shear capacity. The shear model adopted in ACI 440.1R-22[25] is modified to account for the linear elastic behavior and lower modulus of elasticity for FRP reinforcement. CSA S806-12 [26]uses strain-based theory to reflect the effect of FRP reinforcement more effectively, and CSA A23.3-24[27] reflects traditional shear design of steel-reinforced concrete members. The shear capacities predicted by the four design codes were compared with the experimentally determined ultimate loads of each tested beams. The results of this comparison are summarized in Tables 7

and 8.

4.5.2 Comparison of Experimental and Code-Predicted Ultimate Loads

The predicted shear forces were converted into the corresponding applied loads and plotted as horizontal lines on the experimental load-deflection curves, enabling a direct comparison between predicted structural response and the actual structural response.

4.5.2.1 Steel-Reinforced Beams

For steel reinforced beams, the predictions made by the ACI 318-25 and Canadian code CSA A23.3-24 were conservative especially at low concrete compressive strength. ACI 318-25[24] was found to be more consistent with experiment at higher reinforcement ratios. Figures 15 and 16 present a comparison between the experimental results and the predictions of the ACI and CSA codes for steel reinforced beams with concrete compressive strength of 40 MPa and 55 MPa respectively.

4.5.2.2 GFRP-Reinforced Beams

For GFRP-reinforced beams, both ACI 440.1R-22 and CSA S806-12 underestimated the experimental ultimate loads, but the degree of conservatism differed significantly between the two codes. Forecasts made using ACI 440.1R-22 were very conservative. For example, the experimental ultimate load of Beam GC55Re3 was 269.5 kN, whereas ACI 440.1R-22 estimated the ultimate load as 108 kN, which is only half the actual value. A similar trend was observed at lower reinforcement ratios. For Beam GC40Re1, the experimental load of 121 kN was higher than the ACI 440.1R-22 prediction of 89 kN, and CSA S806-12 was slightly higher or identical to the experimental value. Figures 17 and 18 compare GFRP beams with ACI and CSA Codes for both 40 MPa and 55 MPa concrete strength.

5. Conclusions

The following conclusions are drawn from the experimental investigations of twelve reinforced concrete beams without transverse reinforcement:

- Steel- reinforced beams were found to have greater shear capacity and less deflection than GFRP- reinforced beams at the same reinforcement ratios.
- Compared to steel-reinforced beams, the shear capacity of GFRP-reinforced beams was lower by approximately 36% at low reinforcement ratios, 28% at moderate reinforcement ratios, and 16% at higher reinforcement ratios.
- Increasing the concrete compressive strength from 40 MPa to 55 MPa (an increase of 38%) improved the shear capacity of GFRP-reinforced beams more than that of beams reinforced with conventional steel. The shear strength of the GFRP beams increased by 17% and 14% when f'c was increased for ρ_{e2} and ρ_{e3} respectively.
- The shear strength of GFRP-reinforced beams increased by 40% when the reinforcement ratio increased from 0.22% to 0.586%, and by 94% when the reinforcement ratio increased to 1.3%. For the corresponding steel reinforced beams, the increases were 25% and 46% respectively.
- High-strength concrete beams were less affected by their reinforcement ratio with regards to deflection, due to governed the overall beams behavior.
- The ACI code-440.11-22 shear design method was found to be highly conservative when evaluating the shear capacity of GFRP-reinforced concrete beams with an average value 2 for the two selected values of concrete compressive strength.
- In Steel-reinforced beam, the ACI 318-25 design method for shear was found to be conservative by almost 30%

References

[1] A. El-Nemr, E. A. Ahmed, A. El-Safty, and B. Benmokrane, "Evaluation of the flexural strength and serviceability of concrete beams reinforced with different types of GFRP bars," *Eng. Struct.*, vol. 173, Oct. 2018, doi: 10.1016/j.engstruct.2018.06.089.

[2] O. I. Abdelkarim, E. A. Ahmed, H. M. Mohamed, and B. Benmokrane, "Flexural strength and serviceability evaluation of concrete beams reinforced with deformed GFRP bars," *Eng. Struct.*, vol. 186, May 2019, doi: 10.1016/j.engstruct.2019.02.024.

[3] M. Krall and M. A. Polak, "Concrete beams with different arrangements of GFRP flexural and shear reinforcement," *Eng. Struct.*, vol. 198, Nov. 2019, doi: 10.1016/j.engstruct.2019.109333.

[4] I. S. Abbood, S. A. Odaa, K. F. Hasan, and M. A. Jasim, "Properties evaluation of fiber reinforced polymers and their constituent materials used in structures - A review," *Mater. Today Proc.*, vol. 43, no. 2, 2021, doi: 10.1016/j.matpr.2020.07.636.

[5] Hwai-Chung Wu and Christopher D. Eamon, "Strengthening of Concrete Structures Using Fiber Reinforced Polymers (FRP)," Feb. 2017. doi: 10.1016/B978-0-08-100636-8.00001-6.

[6] S. Mousa, H. M. Mohamed, B. Benmokrane, and E. Ferrier, "Flexural behavior of full-scale circular concrete members reinforced with basalt FRP bars and spirals: Tests and theoretical studies," *Compos. Struct.*, vol. 203, pp. 217–232, Nov. 2018, doi: 10.1016/j.compstruct.2018.06.107.

[7] A. Koray Tureyen and Robert J. Frosch,

"Shear Tests of FRP Reinforced Beams," *ACI Struct. J.*, vol. 99, no. 4, Jul. 2002, doi: 10.14359/12111.

[8] S. A. Mohammed and A. M. I. Said, "Analysis of concrete beams reinforced by GFRP bars with varying parameters," *J. Mech. Behav. Mater.*, vol. 31, no. 1, p. 774, Jan. 2022, doi: 10.1515/jmbm-2022-0068.

[9] Antonio Nanni, "Flexural Behavior and Design of RC Members Using FRP Reinforcement," *Journal of Structural Engineering*, vol. 119, Nov. 1993, doi: 10.1061/(ASCE)0733-9445(1993)119:11(3344).

[10] A. El-Nemr, E. A. Ahmed, and B. Benmokrane, "Flexural Behavior and Serviceability of Normal-and High-Strength Concrete Beams Reinforced with Glass Fiber-Reinforced Polymer Bars," *ACI Struct. J.*, vol. 110, no. 6, 2013, doi: 10.14359/51686162.

[11] S. M. H. Rahman, K. Mahmoud, and E. El-Salakawy, "Behavior of Glass Fiber–Reinforced Polymer Reinforced Concrete Continuous T-Beams," *Journal of Composites for Construction*, vol. 21, no. 2, Apr. 2017, doi: 10.1061/(asce)cc.1943-5614.0000740.

[12] G. B. Jumaa and A. R. Yousif, "Predicting shear capacity of FRP-reinforced concrete beams without stirrups by artificial neural networks, gene expression programming, and regression analysis," *Advances in Civil Engineering*, vol. 2018, 2018, doi: 10.1155/2018/5157824.

[13] Y. Sonobe *et al.*, "DESIGN GUIDELINES OF FRP REINFORCED CONCRETE BUILDING STRUCTURES," *Journal of* Composites *for Construction*, vol. 1, no. 3, 1997, doi: 10.1061/(ASCE)1090-0268(1997)1:3(90).

[14] Guilherme S. Melo and Jorge Antonio Rayol, "Shear Resistance of GFRP Reinforced Concrete Beams," 2002, doi: 10.1061/40613(272)5.

[15] S. P. Gross, J. R. Yost, D. W. Dinehart, E. Svensen, and N. Liu, "Shear Strength of Normal and High Strength Concrete Beams Reinforced with Glass Fiber Reinforced Polymer Bars," *American Society of Civil Engineers (ASCE)*, 2003, doi: 10.1061/40691(2003)38.

[16] A. F. Ashour, "Flexural and shear capacities of concrete beams reinforced with GFRP bars," *Constr. Build. Mater.*, vol. 20, no. 10, Dec. 2006, doi: 10.1016/j.conbuildmat.2005.06.023.

[17] Ahmed K. El-Sayed, Ehab F. El-Salakawy, and Brahim Benmokrane, "Shear Strength of Concrete Beams Reinforced with FRP Bars: Design Method," 2005. doi: 10.14359/14875.

[18] F. Abed, H. El-Chabib, and M. Alhamaydeh, "Shear characteristics of GFRP-reinforced concrete deep beams without web reinforcement," *Journal of Reinforced Plastics and Composites*, vol. 31, no. 16, p. 1073, Aug. 2012, doi: 10.1177/0731684412450350.

[19] I. Ali, A. Aziz Abdul Samad, N. Mohamad, G. Al-Kafri, and A. Mohmmed, "Evaluation of shear strength of concrete beams with GFRP reinforcement," *Applied Mechanics and Materials*, vol. 660, 2014, doi: 10.4028/www.scientific.net/AMM.660.603.

[20] Ahmed K. El-Sayed, Ehab F. El-Salakawy, and Brahim Benmokrane, "Shear Strength of FRP-Reinforced Concrete Beams without Transverse Reinforcement," *ACI Mater. J.*, vol. 103, no. 2, 2006, doi: 10.14359/15181.

[21] M. Kaszubska, R. Kotynia, and J. A. O. Barros, "Influence of Longitudinal GFRP Reinforcement Ratio on Shear Capacity of Concrete Beams without Stirrups," in *Procedia Engineering*, Elsevier Ltd, 2017. doi: 10.1016/j.proeng.2017.06.225.

[22] Zdeněk P. Bažant and Qiang Yu, "Designing Against Size Effect on Shear Strength of Reinforced Concrete Beams Without Stirrups: II. Verification and Calibration," *Journal of Structural Engineering*, vol. 131, no. 12, 2005, doi: 10.1061/ASCE0733-94452005131:121886.

[23] L. Jin, X. ang Jiang, H. Xia, F. Chen, and X. Du, "Size effect in shear failure of lightweight concrete beams wrapped with CFRP without stirrups: Influence of fiber ratio," *Compos. B Eng.*, vol. 199, Oct. 2020, doi: 10.1016/j.compositesb.2020.108257.

[24] American Concrete Institute, "ACI 318-25: Building Code Requirements for Structural Concrete and Commentary," American Concrete Institute, Farmington Hills, MI, 2025.

[25] ACI Committee 440, "Building code requirements for structural concrete reinforced with glass fiber-reinforced polymer (GFRP) bars : code and commentary," American Concrete Institute, Farmington Hills, MI, 2022.

[26] "Design and construction of building components with fibre-reinforced polymers," Toronto, ON, Mar. 2012.

[27] "Design of concrete structures," Toronto, ON, Jul. 2024.

أداء قوة مقاومة القص لعتبات الخرسانة المسلحة بألياف زجاجية بدون تسليح القص

الملخص

تهدف هذه الدراسة إلى فحص تأثير قضبان GFRP الطولية على مقاومة القص في العتبات الخرسانية البسيطة المدعومة بدون تسليح في الجدار، ودراسة تأثير التسليح على مقاومة القص. ولتحديد تأثير مقاومة الخرسانة للضغط، ونوع التسليح، ونسبة التسليح على سلوك القص، أُجري برنامج تجريبي على ١٢ عينة من العتبات، شملت ست عتبات مُسلحة تقليديًا بالفولاذ، وست عتبات مُسلحة بقضبان GFRP. وتم استخدام ثلاث نسب تسليح شد مختلفة (منخفضة، متوسطة، وعالية) في كل مجموعة فرعية. صُممت العتبات المُسلحة بقضبان GFRP أو الفولاذ بحيث يكون لها نظريًا نفس قوى الشد ($As\ fy$ ، أو ما يعادلها من خصائص GFRP)، مما أدى إلى قدرة انحناء متقاربة ومقاومتين مختلفتين للخرسانة للضغط. أظهرت النتائج التجريبية أن مقاومة القص للعتبات المُدعمة بألياف زجاجية مُقوّاه بالبوليمر (GFRP) كانت أقل بنسبة ٣٦٪ تقريبًا من مقاومة القص للعتبات المُدعمة بالفولاذ عند نسب التسليح المنخفضة، و٢٨٪ عند نسب التسليح المتوسطة، و١٦٪ عند نسب التسليح العالية. كما أن زيادة مقاومة الخرسانة للضغط من ٤٠ ميجا باسكال إلى ٥٥ ميجا باسكال (٣٨٪) زادت مقاومة القص للعتبات المُدعمة بألياف زجاجية مُقوّاه بالبوليمر (GFRP) بشكل ملحوظ أكثر من العتبات المُدعمة بالفولاذ التقليدي. بالإضافة إلى ذلك، فإن معادلات مدونة المعهد الخرسانة الأمريكية ACI-440.11-22 تُقلل بشكل كبير من تقدير مقاومة القص، حيث بلغ متوسط قيمتها ٢ لقيمتي مقاومة الخرسانة للضغط اللتين تم اختيارهما.

الكلمات المفتاحية

قضبان GFRP، قوة مقاومة القص، حديد القص، فعل الدوّل، نسبة تقوية مقاومة الشد.

Table 1: Properties of fine and coarse aggregate

Physical Properties	Fine Aggregate	Coarse Aggregate
Absorption %	2.08	1.73
Bulk specific gravity, Dry	2.63	2.55
Bulk specific gravity, SSD	2.69	2.60
Apparent specific gravity	2.79	2.67
Dense dry density Kg/m^3	-	1642.64
Fineness Modulus	2.90	-

Table 2: Proportion of concrete mix design for m3

Concrete Type	Cement (kg/m^3)	Fine Aggregate (kg/m^3)	Coarse Aggregate (kg/m^3)	Water (kg/m^3)	W/C ratio	Superplasticizer (kg/m3)
55 MPa	495	704	935	163.35	0.33	4.95
40 MPa	408	730.44	1045	176	0.43	0

Table 3: Beam details

Group	Beam No.	Beam Name	Concrete compressive Strength (MPa)	Reinforcement Type	Reinforcement Ratio (ρ)	No. of Bars and Bar Diameter (mm)
G1	1	SC40Re1	40	Steel	0.00370	5φ 10
	2	SC40Re2			0.01020	7φ 14
	3	SC40Re3			0.01400	10φ 14
G2	4	GC40Re1	40	GFRP	0.00220	3φ 10
	5	GC40Re2			0.00586	4φ 14
	6	GC40Re3			0.01300	9φ 14
G3	7	SC55Re1	55	Steel	0.00370	5φ10
	8	SC55Re2			0.01020	7 φ 14
	9	SC55Re3			0.01400	10φ 14
G4	10	GC55Re1	55	GFRP	0.00220	3φ 10
	11	GC55Re2			0.00586	4φ 14
	12	GC55Re3			0.01300	9φ 14

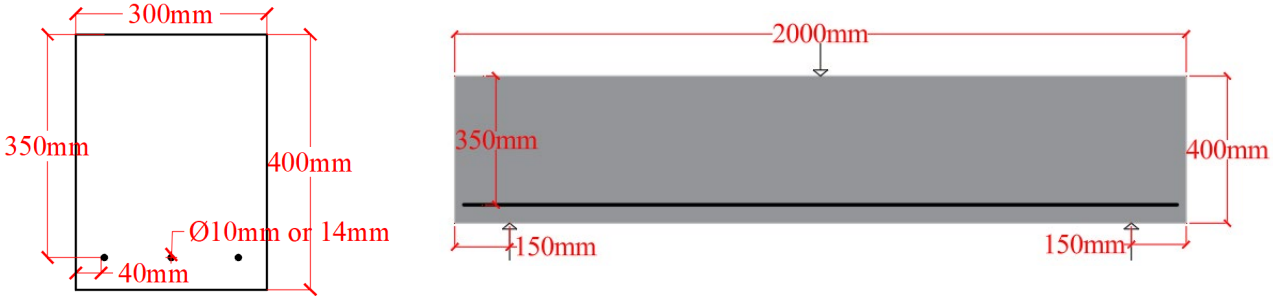

Figure 1: Sketch and cross section of the beams

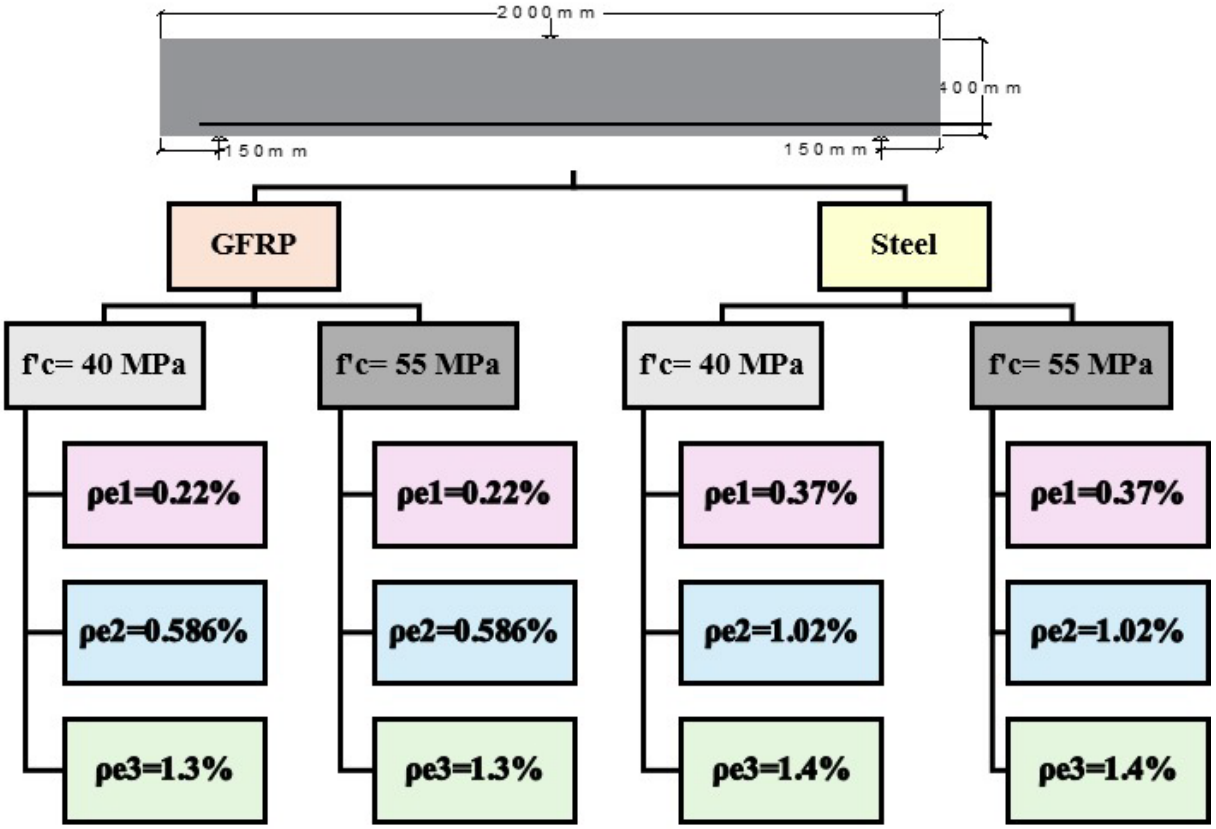

Figure 2: Experimental program flow Chart

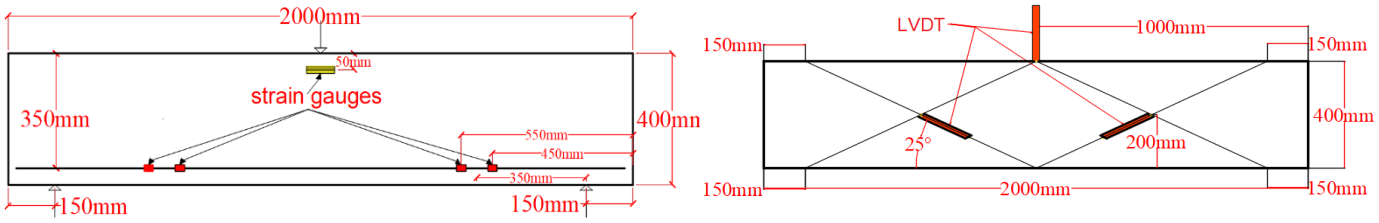

Figure 3: Strain gauges and LVDT location

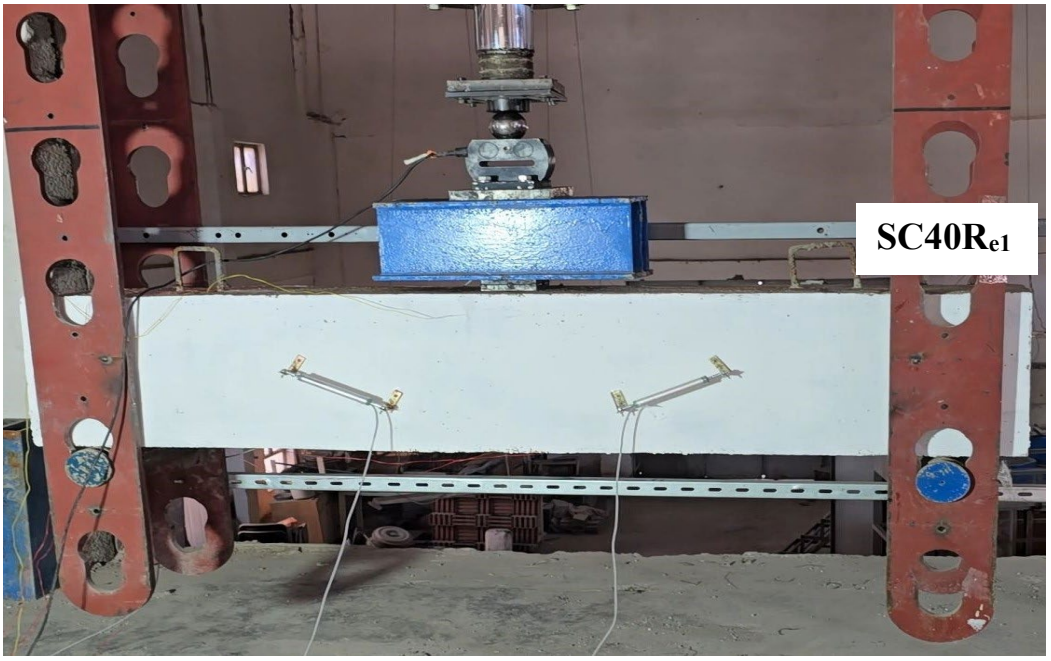

Figure 4: Beam loading and instrument arrangement

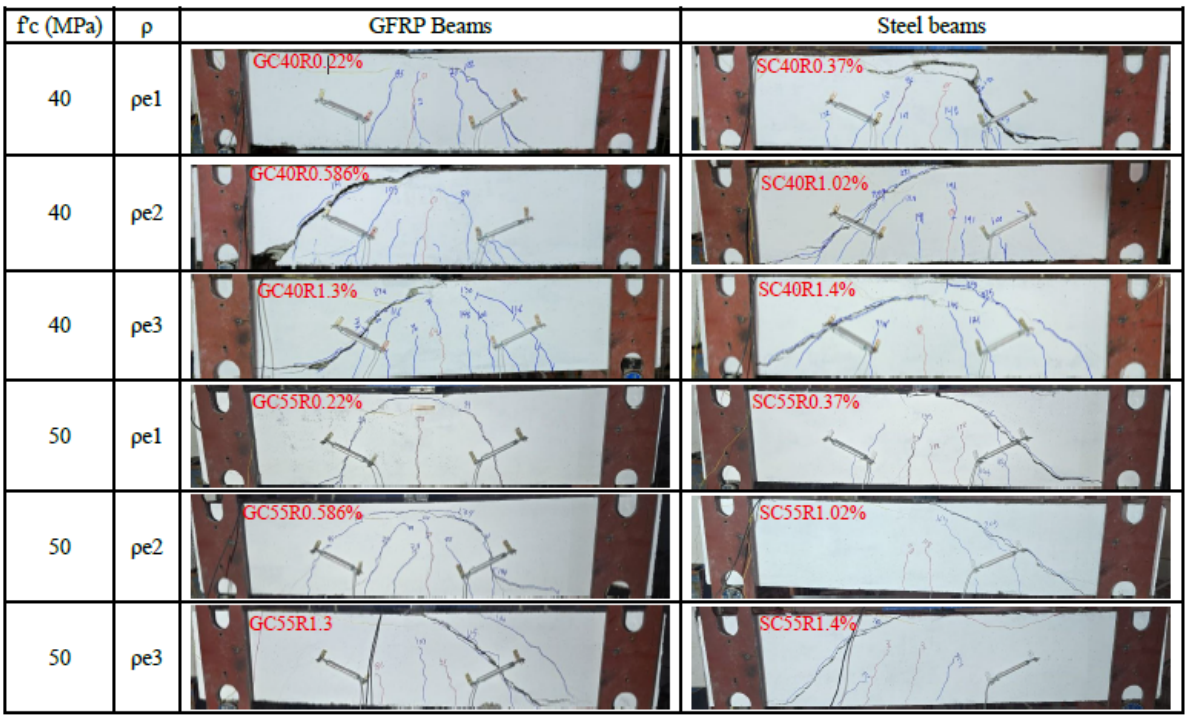

Figure 5: Failure modes of beams

Table 4: Properties of GFRP bars provided by manufacturer

Property	**GFRP**
Material	Fiberglass soaked in a polymer based on epoxy resin
Ultimate tensile strength (MPa)	1200
Modulus of elasticity (MPa)	55,000
Elongation (%)	2.2
Corrosion resistance	Not subjected to corrosion
Heat conduction	Not heat-conductive
Electrical conductivity	Non-conductive (dielectric)
Produced bar diameters (mm)	4 – 20
Length	According to customer request
Environmental impact	Non-toxic; belongs to hazard class 4 (low hazard)
Longevity	Predicted service life of at least 80 years

Table 5: First crack and failure load of beams

Beam Group	Beam No.	Beam ID	Reinforcement Type	First Crack Load (kN)	Failure Load (kN)	Failure Mode	Failure Image
G1	1	$SC40R_{e1}$	Steel	66	190	Shear-Tension	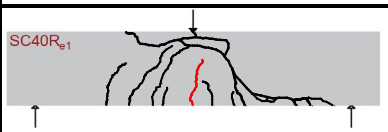
	2	$SC40R_{e2}$		69	237	Shear-Tension	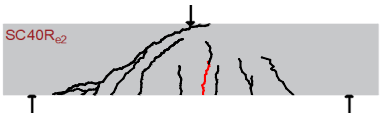
	3	$SC40R_{e3}$		89	279	Shear-Tension	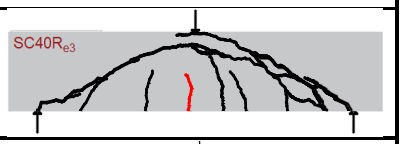
G2	4	$GC40R_{e1}$	GFRP	53	12	Shear-Flexural	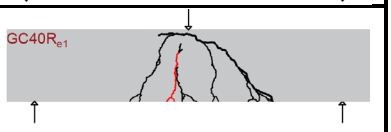
	5	$GC40R_{e2}$		61	170	Shear-Tension	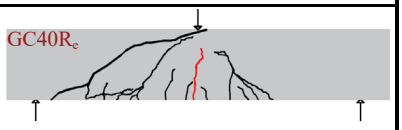
	6	$GC40R_{e3}$		64	235	Shear-Tension	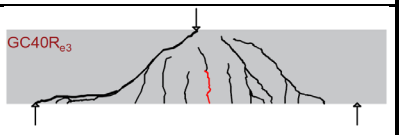
G3	7	$SC55R_{e1}$	Steel	108	204	Shear-Tension	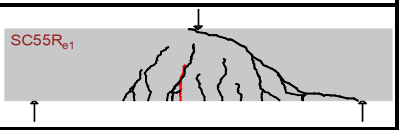
	8	$SC55R_{e2}$		135	265	Shear-Tension	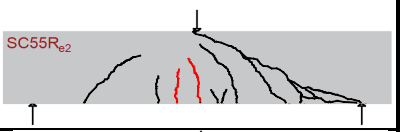
	9	$SC55R_{e3}$		118	279	Shear-Tension	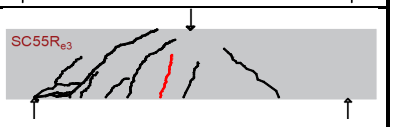
G4	10	$GC55R_{e1}$	GFRP	28	84	Shear-Flexural	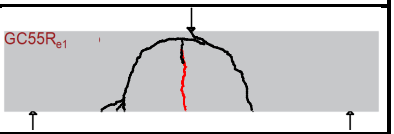
	11	$GC55R_{e2}$		44	199	Shear-Tension	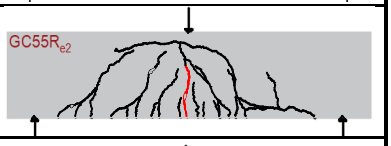
	12	$GC55R_{e3}$		46	269	Shear-Tension	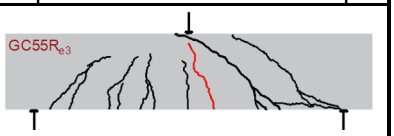

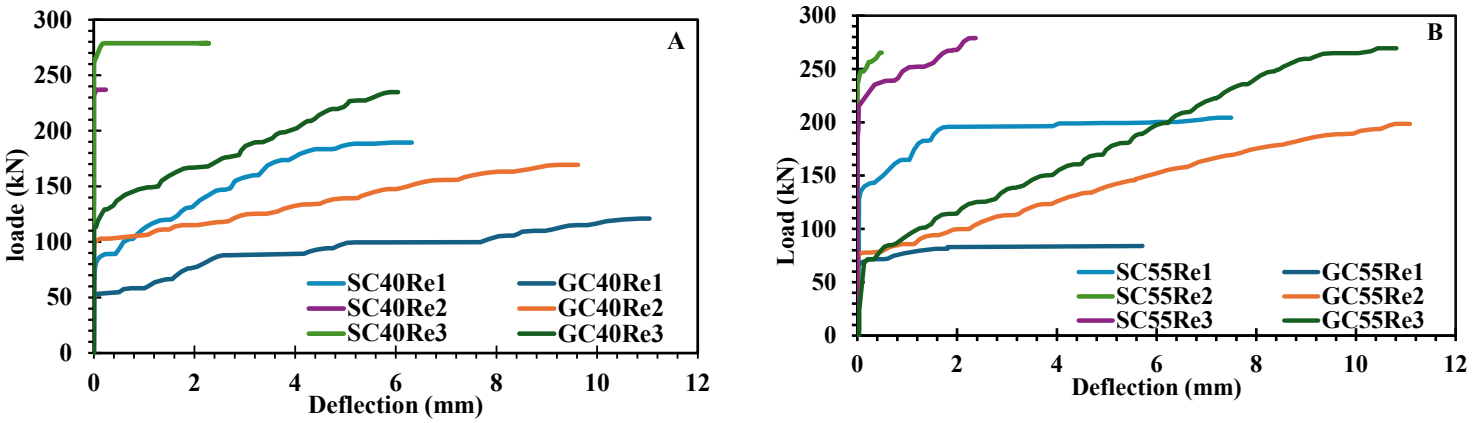

Figure 6: Load deflection curves for steel and GFRP beams, A) 40 MPa concrete compressive strength, B) 55 MPa concrete

Table 6: Mid span deflection and maximum strength

Beams group	Beam No.	Beam ID	f′c (MPa)	Reinforcement Type	ρ (%)	Maximum Load (kN)	Maximum Deflection (mm)
G1	1	$SC40R_{e1}$	40	Steel	0.370	190	6.32
	2	$SC40R_{e2}$			1.020	237	0.24
	3	$SC40R_{e3}$			1.400	279	2.29
G2	4	$GC40R_{e1}$	40	GFRP	0.220	121	11.04
	5	$GC40R_{e2}$			0.586	170	9.62
	6	$GC40R_{e3}$			1.300	235	6.05
G3	7	$SC55R_{e1}$	55	Steel	0.370	204	7.50
	8	$SC55R_{e2}$			1.020	265	0.486
	9	$SC55R_{e3}$			1.400	279	2.37
G4	10	$GC55R_{e1}$	55	GFRP	0.220	84	5.72
	11	$GC55R_{e2}$			0.586	199	11.08
	12	$GC55R_{e3}$			1.300	269	10.81

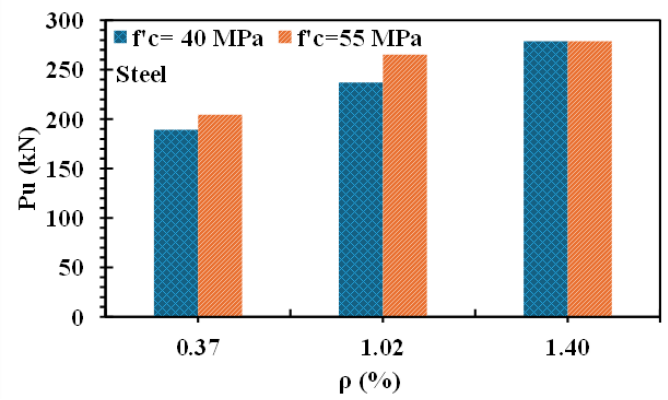

Figure 7: Steel beams with two different compressive strengths

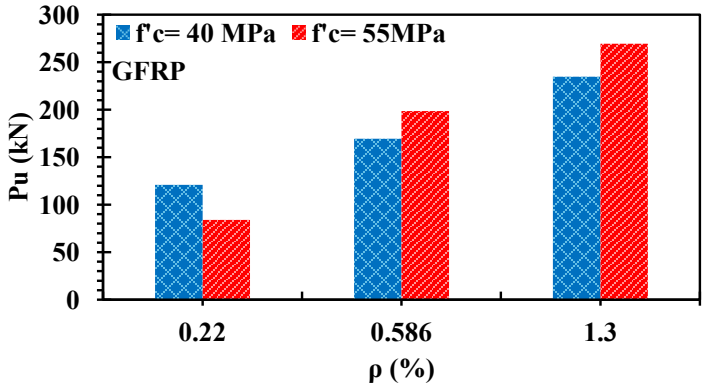

Figure 8: GFRP beams with two different compressive strengths

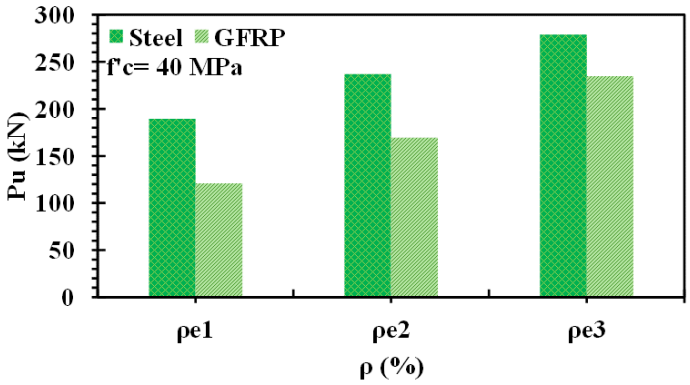

Figure 9: Results for two different types of reinforcement in 40 MPa concrete compressive strength

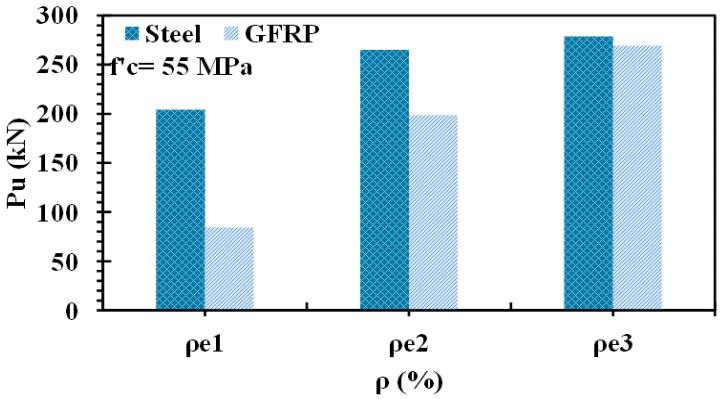

Figure 10: Comparison of two different reinforcement type at 55 MPa compressive strength

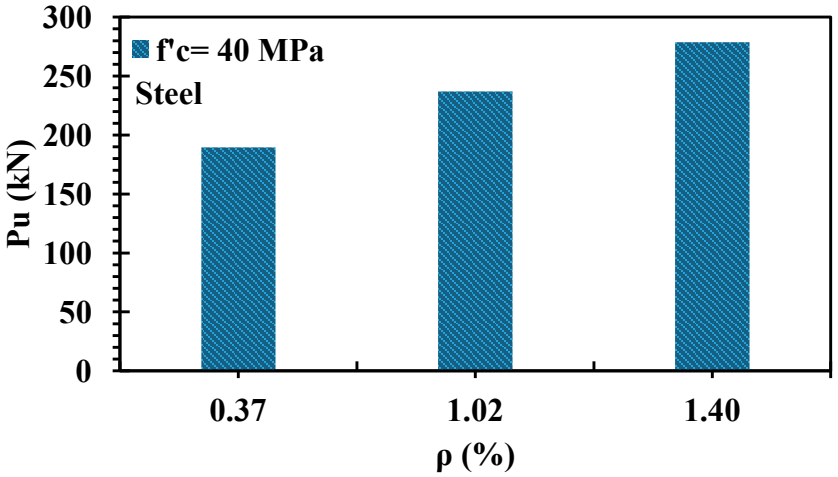

Figure 11: Bar chart of steel beams with different reinforcement ratios at 40 MPa concrete strength

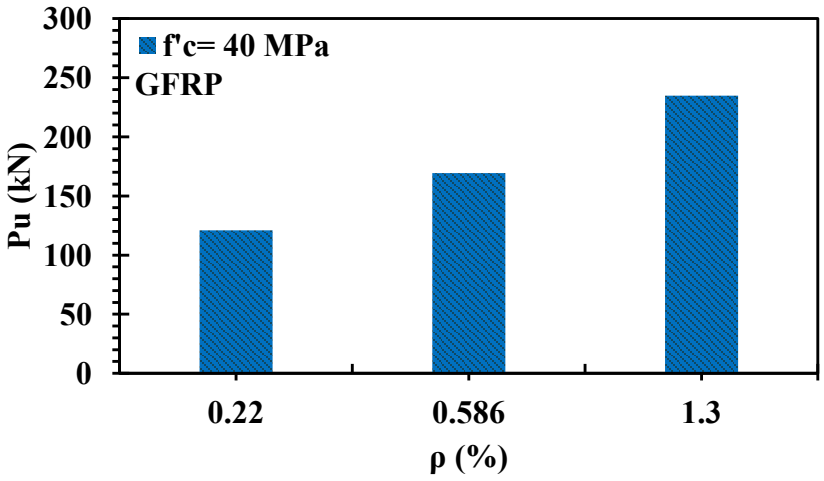

Figure 12: Bar chart of GFRP beams with different reinforcement ratios at 40 MPa concrete strength

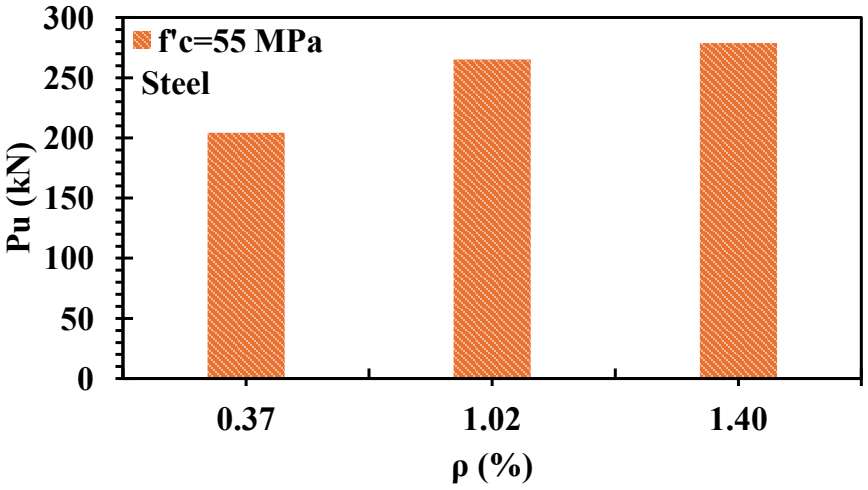

Figure 13: Bar chart of steel beams with different reinforcement ratios at 55 MPa concrete strength

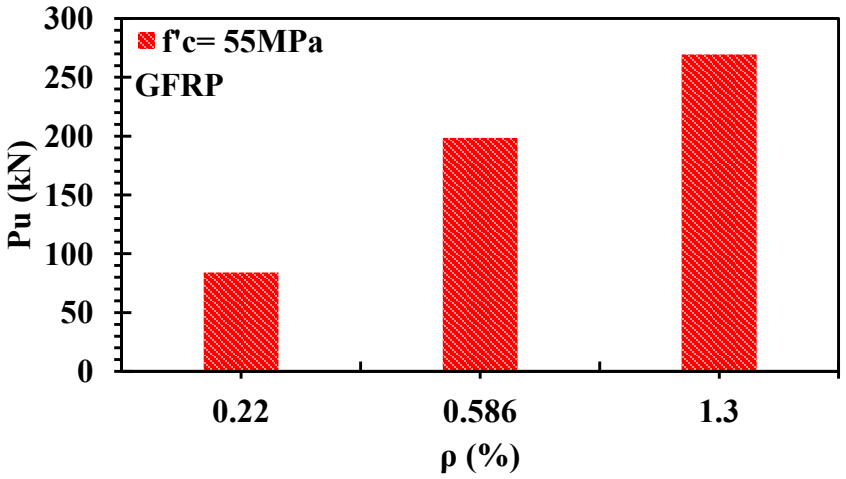

Figure 14: Bar chart of GFRP beams with different reinforcement ratio at 55 MPa concrete strength

Table 7: ACI and CSA equations for shear strength

Code	Equation for Shear Strength, V_c	Notes / Parameters
ACI 318-25 (Steel RC, $Av < Av\_min$)	$V_c = 0.66\lambda_s\lambda\sqrt[3]{\rho_w}\sqrt{f'_c}b_w d$	λ: lightweight factor (1.0 for normal) λ_s: size effect, $\rho_w = As/(bwd)$, $f'c$: concrete compressive strength, b_w: web width, d: effective depth
ACI 440.1R-22 (FRP RC)	$V_c = \frac{2}{5}\sqrt{f'_c}\lambda_s k_{cr} b_w d$	k_{cr}: cracking factor, λ_s: size effect, f'_c: concrete strength, b_w and d as above
CSA S806-12 (FRP RC)	$V_c = 0.05\,\lambda\,k_m\,k_r\,\sqrt[3]{f'_c}b_w d_v$	$k_m = \sqrt{\frac{v_f d}{M_f}} \le 1$, $k_r = 1 + (\sqrt[3]{E_f\rho_f})$ $d_v = max(0.9d, 0.7h), \rho_f = A_f/(b_w d)$, E_f: FRP modulus, $b_w, f'c$ as above λ = modification factor for concrete density, $\lambda = 1.00$ for normal density, 0.85 semi-low-density concrete in which all the fine aggregate is natural sand, and 0.75 for structural low-density concrete in which none of the fine aggregate is natural sand
CSA A23:24 (Steel RC)	$V_c = \lambda\beta\sqrt{f_c}b_w d_v$ where $\beta = \frac{0.4}{1+1500\varepsilon_x} x \frac{1300}{1000+s_{ze}}$	ε_x longitudinal strain, $s_{ze} = 35s_z/(15 + a_g) \ge 0.85s_z$, $s_z = d_v$, a_g= aggregate size, d_v =max(0.9d,0.7h), $\lambda = 1$ normal concrete

Table 8: Experimental result with codes result

Beam Designation	P(pred). (kN) ACI318-25	P(pred). (kN) ACI 440-22	P(pred). (kN) CSAS806-2012	P(pred). (kN) CSA23.3-24	Experimental results(kN)	$\frac{P_{exp.}}{P_{(pred.ACI318)}}$	$\frac{P_{exp.}}{P_{(pred.ACI440)}}$	$\frac{P_{exp.}}{P_{(pred.CSA806)}}$	$\frac{P_{exp.}}{P_{(pred.CSA23.3)}}$
SC40Re1	123.77	-	-	127.43	190	1.54	-	-	1.49
SC40Re2	173.5	-	-	131.96	237	1.37	-	-	1.79
SC40Re3	192.86	-	-	131.21	279	1.44	-	-	2.13
GC40Re1	-	89	131.49	-	121	-	1.36	0.92	-
GC40Re2	-	89	157.24	-	170	-	1.91	1.08	-
GC40Re3	-	99.38	199.85	-	235	-	2.36	1.18	-
SC55Re1	145.13	-	-	148.75	204	1.41	-	-	1.37
SC55Re2	203.5	-	-	152.79	265	1.3	-	-	1.72
SC55Re3	226.15	-	-	151.02	279	1.23	-	-	1.85
GC55Re1	-	104.35	154.18	-	84	-	0.81	0.55	-
GC55Re2	-	104.35	174.85	-	199	-	1.91	1.14	-
GC55Re3	-	108.35	222.23	-	269	-	2.48	1.20	-

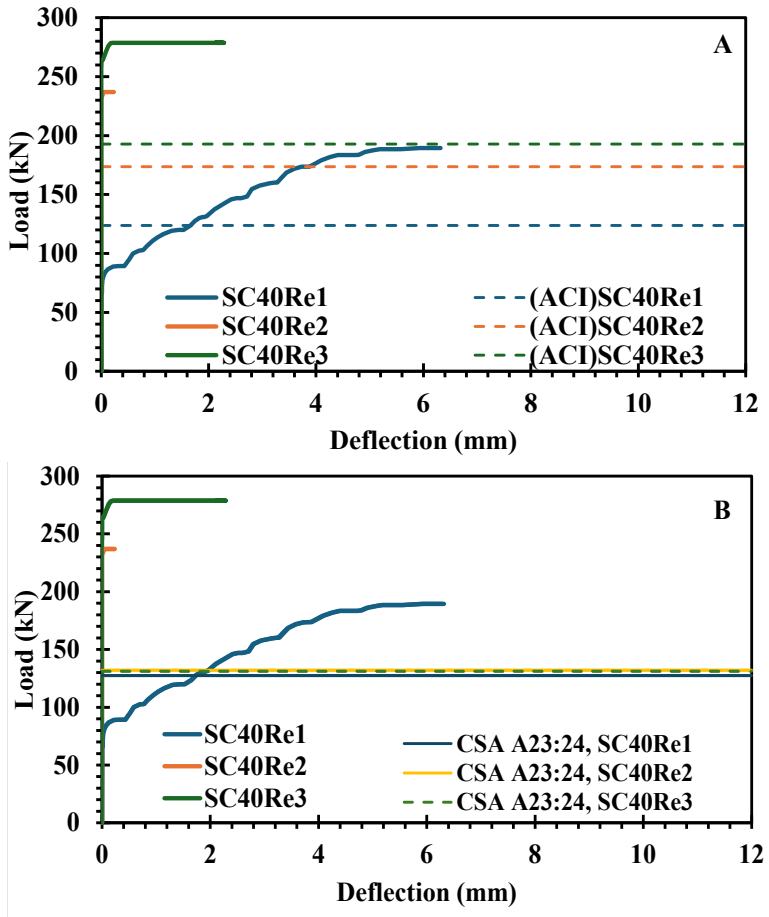

Figure 15: A) ACI code predictions B) Canadian code predictions for 40 MPa concrete steel beams

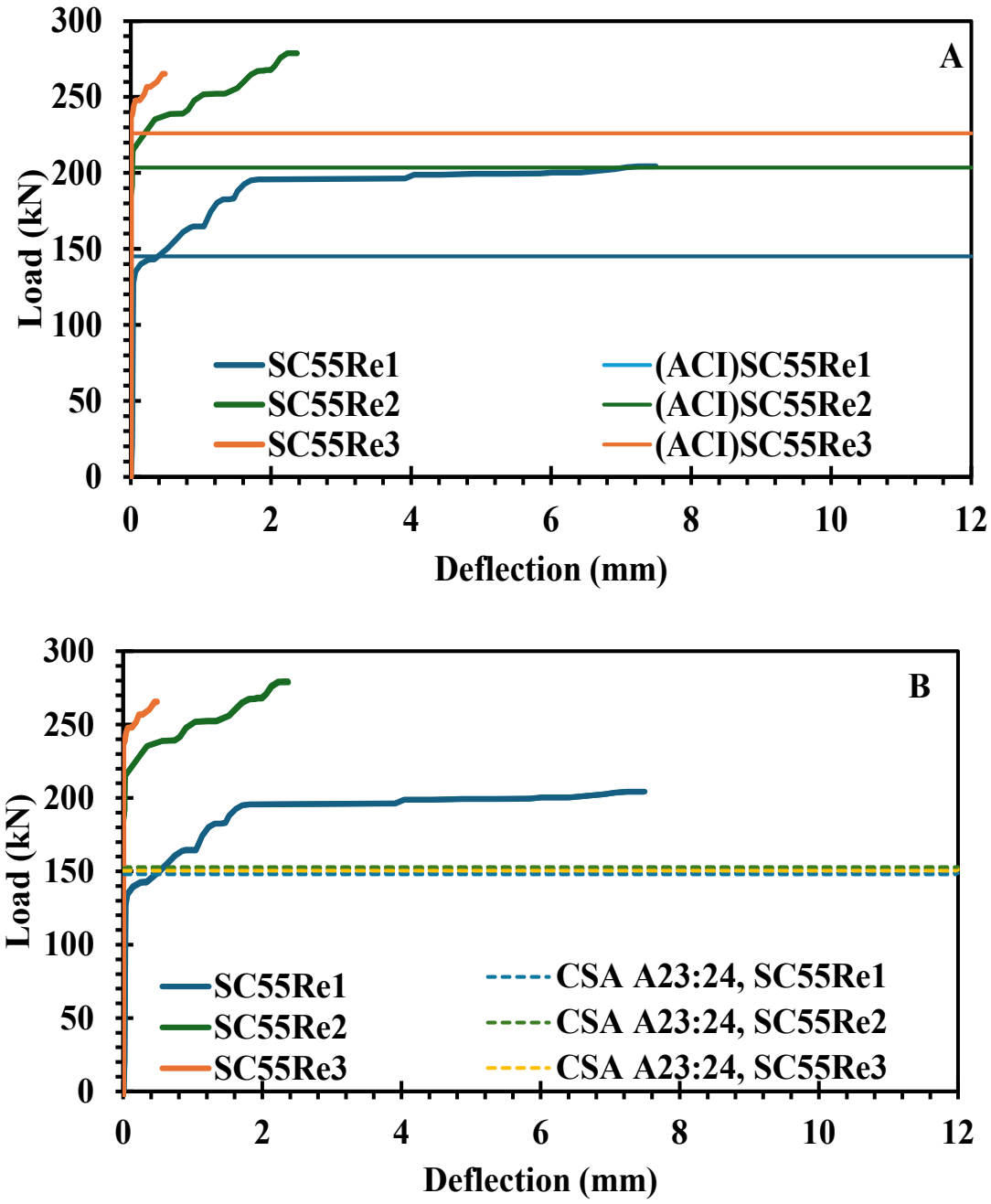

Figure 16: A) ACI code predictions B) Canadian code predictions for 55 MPa concrete Steel beams

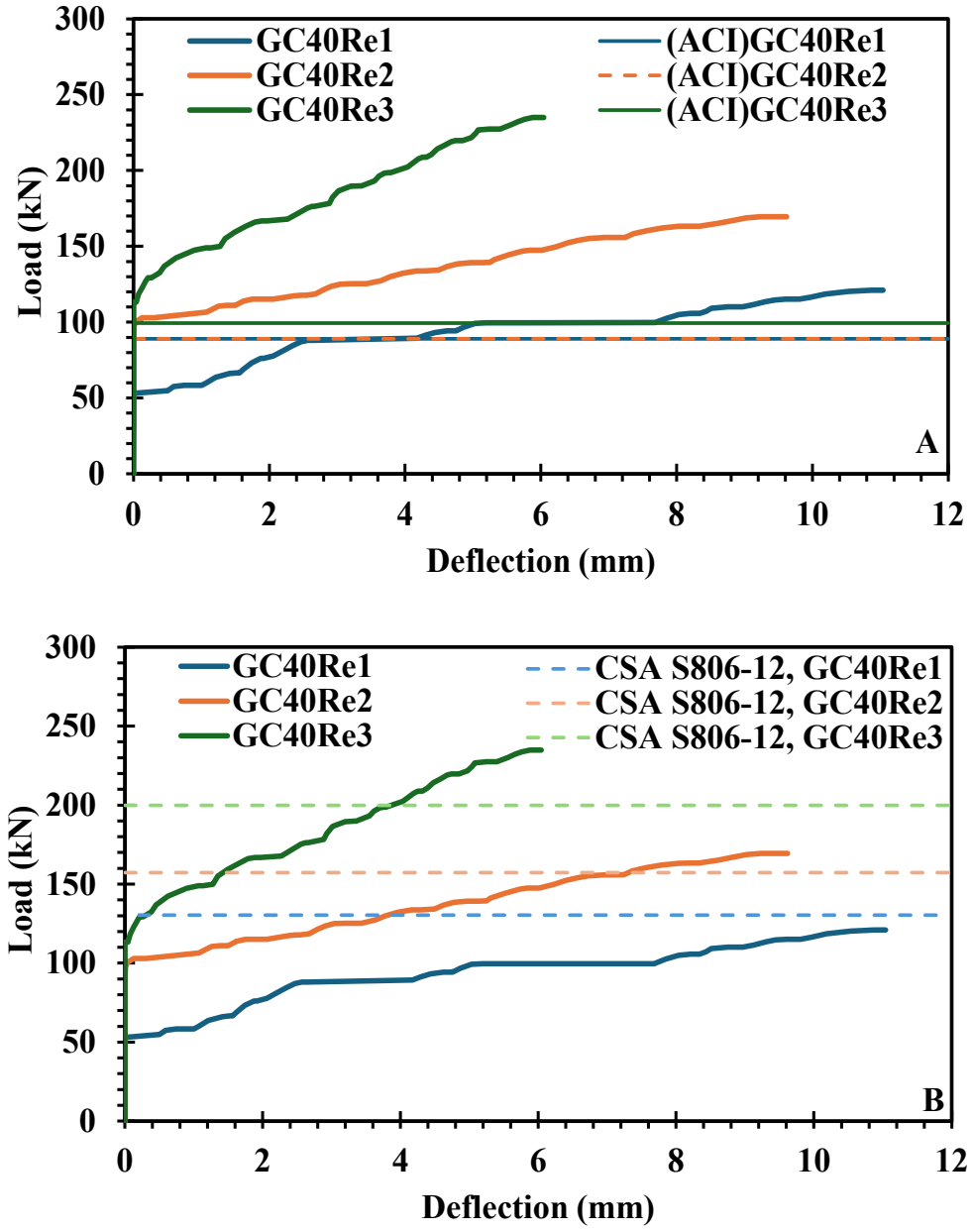

Figure 17: A) ACI code predictions B) Canadian code predictions for 40 MPa concrete GFRP beams

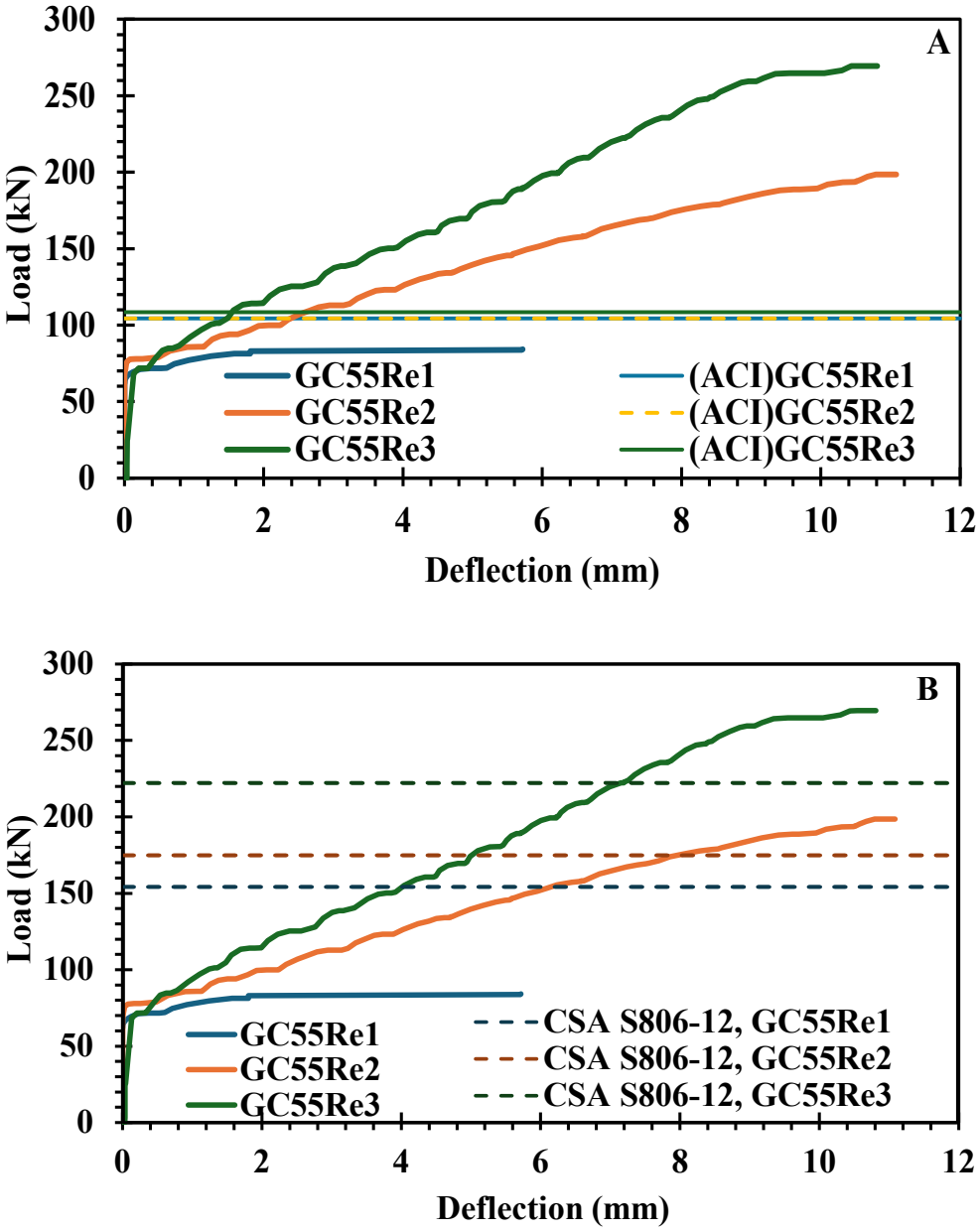

Figure 18: A) ACI code predictions B) Canadian code predictions for 55 MPA concrete GFRP beam